

SIMULATION OF DEFLECTING SYSTEM BASED ON PERMANENT MAGNETS WITH A NON-UNIFORM MAGNETIC FIELD TO REGISTER ACCELERATED AND DECELERATED ELECTRONS GENERATED IN DIELECTRIC LASER ACCELERATOR

I.V. Beznosenko, A.V. Vasyliiev, G.V. Sotnikov

National Science Center "Kharkov Institute of Physics and Technology", Kharkiv, Ukraine

E-mail: beznosenko1989@gmail.com

Deflection system was designed and computed to spatially separate beam of electrons with different energies in the range of several tens of kiloelectronvolts. Three specific cases with electron energies of (33.9 ± 0.3) , (18.2 ± 0.3) , and (14.2 ± 0.3) keV were examined for experiments using Dielectric Laser Accelerators. The results of calculations of the spatial distribution of the magnetic field induced by a pair of permanent magnets and its effect on electrons moving in this field are presented. Such magnetic spectrometers differ from their analogues in that particles do not move along the center between magnets in a uniform magnetic field, but along their periphery, where the field is non-uniform, which provides higher resolution. Presented spectrometer provides the electron energy resolution of less than 10 eV. Research on such systems holds significant importance for the further development of methods for analyzing electrons with varying energies in modern accelerators and spectrometers.

PACS: 41.75.Jv, 41.75.Ht, 42.25.Bs

INTRODUCTION

Currently, there are several schemes for measuring the energy of accelerated electrons. For example, to measure electrons with high energy but high divergence, a stack of metal sheets with scintillators placed between them is often used [1]. This allows the energy of electrons to be measured based on their travel distance in a stack of metal and scintillator. However, in most cases, dipole magnetic spectrometers, which deflect electrons depending on their energy, are used to measure electron energy [2].

Early experiments with Laser Wakefield Accelerators (LWFA) often used image plates [3] because they had high sensitivity and dynamic range. However, they were limited to a single dimension or integration over multiple dimensions and were not suitable for high-frequency experiments or statistical studies of electron beams, such as in dielectric laser accelerator (DLA) experiments. With the development of technology and the standardization of the production of dense quasi-mono-energy electron beams, spectrometers are increasingly equipped with scintillation screens captured using cameras.

A dipole magnetic spectrometer works by deflecting electron trajectories depending on their energy. The energy resolution limit is reached when the separation of the two energies is equal to the cross-sectional size of the electron beam. Resolution is limited by the size of the beam in the object plane of the magnet, as well as possible focusing aberrations within the magnet and limitations in electron detection.

Dielectric laser accelerators are attracting increasing attention from researchers due, first of all, to their super compactness [4]. But obtaining required for DLA short bunches of electrons, which are limited in time of acceleration in an electric field, is a difficult task from a scientific and technical point of view [5]. The length of the electron bunches must be less than the length of the accelerating phase of laser radiation. For example, if we

consider laser radiation with a wavelength of 800 nm and want to accelerate relativistic electrons, then the length of the electron bunch should not exceed a quarter of the wavelength (200 nm). This is due to the need to maintain long-term synchronism between the accelerated electrons and the laser radiation field. Moreover, it is necessary to ensure such a delay of the bunch that this bunch of electrons is accurately injected into the accelerating phase of laser radiation.

Currently, obtaining the short bunches required for DLA is problematic. Therefore, to measure and analyze the acceleration rates of electrons accelerated through various DLA structures, solutions, which allow spatial separation of accelerated and decelerated electrons, are used [6]. Such electrons come out of the DLA if a long bunch of electrons (more than half the wavelength of laser radiation) passes through the dielectric chip structure. This is due to the fact that some parts of this bunch are injected into the accelerating phase of the laser radiation, and others are injected into the decelerating phase. As a consequence, different electrons in this bunch are accelerated and decelerated to different extent by the field excited by laser radiation above the structure. In this case, separation is achieved by using magnetic spectrometers. In experiments on the acceleration of nonrelativistic particles [7] researchers carry out measurements, and the paper [8] describes the use of a spectrometer developed by the authors with a resolution of 40 eV. You can also evaluate the resolution by measuring the dispersion of the mass spectrometer, which is determined by the distance between the maxima of the distributions of particles with different masses. According to [2], the dispersion of the mass spectrometer, calculated on the basis of the distance between the distribution maxima of two thallium isotopes, is 11.5 mm with a mass difference of 1%. Such dispersion is also observed for electrons with different relativistic masses:

$$m_{rel} = m_0 \cdot \gamma = m_0 \cdot \left(1 + \frac{E_k}{E_0}\right), \quad (1)$$

where $m_0 = 9.1 \cdot 10^{-31}$ kg is electron rest mass; γ is Lorentz factor; E_k is electron kinetic energy; $E_0 = 511$ keV is electron rest energy.

According to equation (1), the relativistic mass of an electron with an initial energy approaching 30 keV, after an assumed acceleration process of about 300 eV [6], will be slightly different from the relativistic mass of a similar electron that has undergone deceleration. The difference in mass is only 0.11%. However, under these conditions, the dispersion of the mass spectrometer is insufficient to accurately determine the acceleration rate with an accuracy of better than 13%.

To analyze successfully acceleration rates in our experiments [9], it is necessary to increase the resolution of the mass spectrometer to a level that provides an accuracy of no worse than 10 eV. As will be shown below, this accuracy follows from a numerical analysis of the electron beam trajectories in the proposed experiment scheme.

1. PROBLEM FORMULATION

A setup scheme for conducting experiments on dielectric laser acceleration of electrons in periodic chip structures (diffraction gratings of various profiles [9]) is presented in Fig. 1. The main purpose of the setup is to study the processes of acceleration of electron beams of various initial energies.

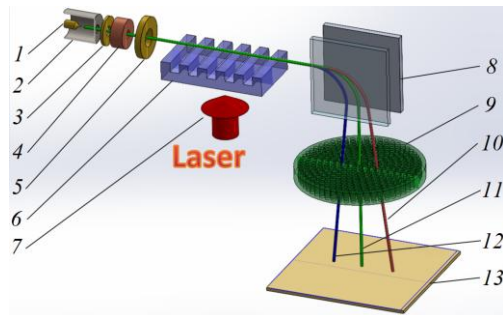


Fig. 1. Scheme of the experimental setup for dielectric laser acceleration on a periodic structure:

- 1 is thermal cathode nanotype; 2 is modulator (venelt);
- 3 is accelerating anode; 4 is focusing system;
- 5 is anode, 6 is periodic structure; 7 is laser radiation;
- 8 is deflecting magnets; 9 is MCP; 10 is accelerated electrons; 11 is electrons with initial speed;
- 12 is decelerated electrons; 13 is phosphorus screen

An electron beam with a given initial energy is formed using an electron gun consisting of a thermionic cathode, nanotype (1), modulator (2), accelerating anode (3), focusing system (4) and anode (5). Next, electrons are injected into a modulated periodic electromagnetic field created by a laser pulse (7) passing through a periodic structure (6). The length of the electron beam significantly exceeds the wavelength of laser radiation. Therefore, at this stage, beam electrons injected in the accelerating phase of the field increase its energy and beam electrons injected in the decelerating phase decrease its energy. Thanks to this, at the output from the laser accelerator we obtain a spectrum of electrons with different energies, both accelerated and decelerated. To analyze the efficiency of acceleration, it is necessary to determine their energies. For this purpose, flat deflect-

ing magnets (8) are used, which spatially separate electrons with different energies. In a magnetic field, due to the difference in Larmor radii value, electrons are separated into accelerated (10), with initial energy (11) and decelerated electrons (12). The goal of our work is also to obtain such a resolution of the magnetic spectrometer that will make it possible to detect the presence of particles with intermediate energy values within each group of accelerated and decelerated electrons. It is assumed that the number of electrons in the beam during the duration of the laser pulse will be small, so spatially separated electrons pass through the MCP (9) in order to increase the output signal on the phosphorus screen (13).

In a uniform magnetic field, an electron makes a circular motion with a Larmor radius [10]:

$$R = \frac{m_0}{B \cdot e} \cdot \sqrt{\left(\frac{E_k}{m_0 \cdot c^2} + 1\right)^2 - 1}, \quad (2)$$

where $c = 3 \cdot 10^8$ m/s is speed of light; $e = 1.6 \cdot 10^{-19}$ C is electron charge; B is magnetic induction (T).

I.e. knowing the radius of the deflected electron R (and hence the shift of the electron on the registration screen) and the magnetic induction B from expression (2), we can unambiguously determine the energy of the electron E_k . As follows from expression (2), the resolution of the spectrometer (change in radius) ΔR is proportional to the change in magnetic induction ΔB .

In a non-uniform magnetic field, it is impossible to obtain an explicit analytical dependence of the electron deflection on the magnitude of the magnetic induction. To find it, it is necessary to solve numerically the equations of motion of an electron with a given initial energy in a given constant magnetic field. We use block magnets to deflect electrons. The spatial distribution of magnetic induction is found by numerically solving the magneto-static problem. The found numerical solution can be compared with the analytical expression on the axis of a pair of permanent magnets, the magnetic induction of each is described by the expression (Fig. 2) [11, 12]:

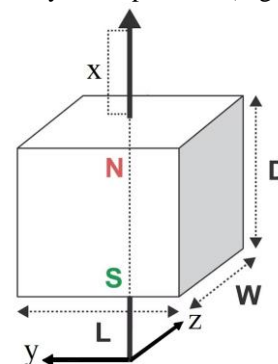


Fig. 2. Rectangular permanent magnet and its dimensions: N is north pole of the magnet; S is south pole of the magnet

$$B = \frac{B_r}{\pi} \cdot \left[\arctan \left(\frac{L \cdot W}{2 \cdot x \cdot \sqrt{4 \cdot x^2 + L^2 + W^2}} \right) - \arctan \left(\frac{L \cdot W}{2 \cdot (D+x) \cdot \sqrt{4 \cdot (D+x)^2 + L^2 + W^2}} \right) \right], \quad (3)$$

where B_r is remanence field; x is distance from a pole face on the symmetry axis; L is length of the block; W is width of the block; D is thickness (or height) of the block.

From equation (3) it follows that the magnetic field in the plane between the magnets increases with increasing geometric dimensions of the magnets and remanence, but decreases with increasing distance between the magnets. From (2) it follows that electrons in this plane will be deflected more strongly with increasing the intensity of a magnetic field and with decreasing their energy.

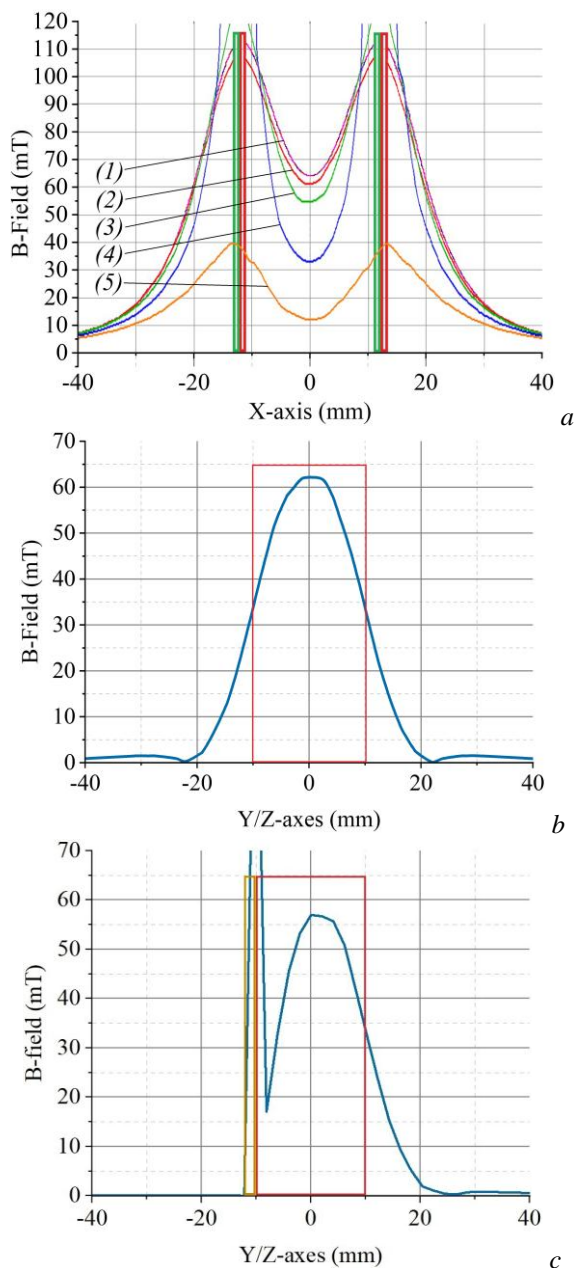


Fig. 3. Distribution of the magnetic induction modulus between two magnets (here the origin of coordinates is at the point $x=0, y=0, z=0$): (a) is distribution graph along the X-axis: analytical dependence according to equation (3) at $y=0$ (1), numerical solutions at $y=0$ (2), at $y=5$ (3), at $y=10$ (4) and at $y=15$ (5); (b) is distribution graph along the Y- or Z-axis at $x=0$ without steel plates; (c) is distribution graph along the Y- or Z-axis at $x=0$ with steel plates

Fig. 3 shows the distribution of the magnetic induction modulus B along the X-, Y-, and Z-axes for a deflecting system of two rectangular magnets ($D = 2$ mm, $L = 20$ mm, $W = 20$ mm). For the calculations, we used neodymium magnets of Grade № 35 with remanence $B_r = 1.17$ T [12] and with a distance between them along the X-axis equal to 22.5 mm. The red and green frames respectively indicate the locations of the north (N) and south (S) poles of the magnets, the yellow frames indicate the steel plates (screens) needed to compensate for the long-range deflecting magnetic field in the path of the electrons. In Fig. 3, the origin of the coordinate system is located at the center between the magnets (Fig. 4).

Fig. 3 shows the distribution of the magnetic induction modulus between two magnets under various conditions, including the presence and absence of steel plates (screens), which plays an important role in controlling the trajectories of electrons. Fig. 3,a shows a graph of the distribution of magnetic induction along the X-axis for various values of y . The first curve (1) represents the analytically calculated distribution of magnetic induction at $y=0$, according to equation (3). Next, numerical solutions are presented for various values of y (everywhere $z=0$): curve 2 at $y=0$, curve 3 at $y=5$, curve 4 at $y=10$ and curve 5 at $y=15$. When comparing the results of analytical (1) and numerical calculations (2), we can conclude that the analytically calculated magnetic induction is consistent with its numerical solutions. Fig. 3,b shows the distribution of the magnetic field along the Y- or Z-axis at the center between the magnets at $x=0$, when there are no steel plates. In this case, the magnetic field has a distribution with the reverse magnetic field, which changes the direction of movement of electrons to the opposite when they approach the edges of the magnets. In order to suppress the reverse magnetic field, steel plates made of 1008 steel are installed in our spectrometer. Plate dimensions: height is 20 mm, width is 90 mm, thickness is 2 mm. Fig. 3,c shows a graph illustrating the distribution of the magnetic induction modulus on the Y- or Z-axis, also at $x=0$, but with the presence of steel plates. The first peak of magnetic induction, which reaches 125 mT, is located inside the steel plate and does not have a significant effect on the trajectory of the electrons.

2. CALCULATION OF MAGNETIC DEFLECTION SYSTEM

In the experiment to study the acceleration of electrons in DLA, developed at the National Scientific Center KIPT [13], the maximum increase in electron energy is expected at a level of approximately 300 eV. Therefore, in order to achieve registration of maximally accelerated/decelerated electrons, as well as electrons with intermediate energies, it is necessary to obtain electron divergence angles that allow for an energy resolution of the order of 10 eV. For these purposes, we have developed a deflection system consisting of two permanent magnets. These magnets were placed at a certain distance from each other so that the trajectory of electrons with initial energy changed its angle by 90 degrees in the YZ-plane (Fig. 5). The choice of this trajectory con-

figuration was also determined by the location of the registration device, which position remained fixed during the experiment.

In order for electrons to move in the YZ-plane at each moment of time, the electron beam must pass strictly in the center between the magnets and be equidistant from each magnet. This is because the direction of the Lorentz force is perpendicular to the direction of movement of electrons and to the direction of the magnetic field lines shown in Fig. 4. The magnetic field indicated by green arrows (in the center of the vertical axis between the magnets) is several tens of times more intense than the field indicated by blue arrows (at the edges of this axis when the field changes its direction).

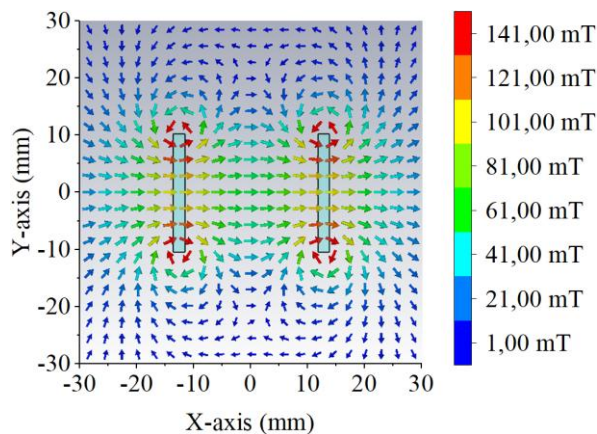


Fig. 4. Magnetic field lines between two permanent magnets in the XY-plane at $z=0$

Since magnetic induction is spatially non-uniform, the particle in cell simulation method was used to simulate the movement of electrons with different energies.

First, it was simulated a situation in which a beam of electrons with a diameter of $3 \mu\text{m}$ after the accelerating system was directed along the center of the space between the previously described magnets. After moving in the perpendicular direction by a distance of 190 mm (for the designation see Fig. 6), after passing the magnets, decelerated electrons with $E_{kd} = 33.6 \text{ keV}$ and accelerated electrons with $E_{ka} = 34.2 \text{ keV}$ were separated by a distance of 2.5 mm. That is, their divergence after coming out of the magnetic field was 13 mrad.

Then it was simulated a situation (see Fig. 6), where the electron beam was directed parallel to the previous direction, but shifted vertically (along the Y-axis) by 8 mm relative to the center of the magnets. With such a shift, it was possible to change the trajectory of the electrons by 90° again. Now, at a distance of 190 mm after the magnets, decelerated electrons with $E_{kd} = 33.6 \text{ keV}$ and accelerated electrons with $E_{ka} = 34.2 \text{ keV}$ were separated by a distance of 3.5 mm. That is, their divergence after coming out of the magnetic field was 17 mrad.

At other shifts, the trajectory of the electrons was not changed by 90° , which means the electrons did not hit the microchannel plate (MCP). Thus, it was found that under the same conditions, there are only two parallel initial paths for electrons, in which they can change their trajectory in the magnetic field of a pair of permanent magnets to the same angle.

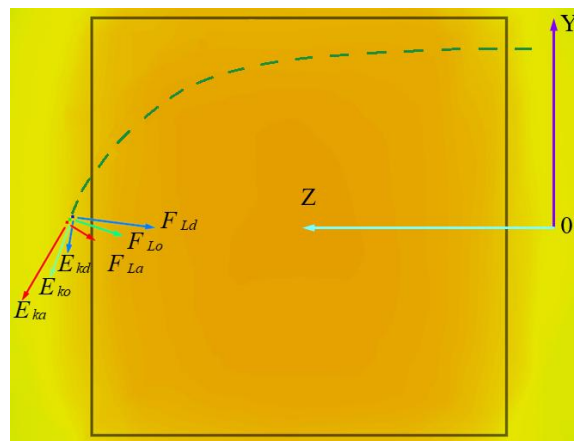


Fig. 5. Trajectories of decelerated electrons E_{kd} , electrons moving with an initial speed E_{ko} and accelerated electrons E_{ka} in a magnetic field (magnets are indicated by a gray frame) and the directions of the Lorentz force \vec{F}_{Ld} , \vec{F}_{Lo} , and \vec{F}_{La} respectively

Since the magnetic field at a certain distance from the magnets along the path of the electrons changed sign (see Fig. 3,b, its description and Fig. 4), the electrons were deflected slightly in one direction, then significantly in the opposite direction and slightly in the first direction again. Thus, the spatial separation of electrons with different kinetic energies when bending the trajectory of their movement in a magnetic field was compensated to some extent. As noted above, in order to suppress the magnetic field, which has the opposite direction along the path of electrons, plates made of 1008 steel were installed (see shown in Fig. 6). It was simulated a situation in which the electron beam was directed parallel to the previous directions, but shifted vertically (along the Y-axis) by 11.4 mm relative to the center of the magnets. That is, initially the beam moved above the pair of magnets by 1.4 mm. With such shift, it was possible to change the trajectory of the electrons by 90° again. Now, at a distance of 190 mm after the magnets, decelerated electrons with $E_{kd} = 33.6 \text{ keV}$ and accelerated electrons with $E_{ka} = 34.2 \text{ keV}$ were separated by a distance of 4.5 mm. That is, their divergence after coming out of the magnetic field was 22 mrad.

Fig. 6 shows the selected configuration of permanent magnets and registering device for the DLA experiment. Electrons move from right to left, and then from top to bottom (see Fig. 6,a) or towards the observer, and then from top to bottom (see Fig. 6,b). The magnets are serial and are widely available. The registering device is an MCP with a resolution of $10 \mu\text{m}$, the center of which along the X-axis lies in the plane of motion of electrons between the magnets, and along the Z-axis lies in the same plane with the far edges of the magnets. MCP is at our disposal. The selected distance between the magnets will provide a suitable magnetic field to bend the trajectory of electrons by 90° and a sufficient divergence between electrons with different kinetic energies (Fig. 7) providing a resolution of the order of less than 10 eV at the selected distance to the MCP, which is related to the dimensions of the experimental setup.

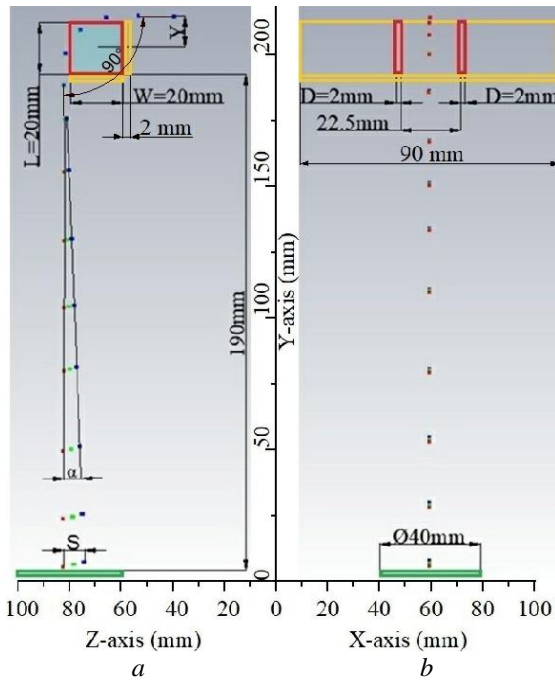


Fig. 6. Numerical model showing the positions of decelerated electrons (blue), electrons with initial energy (green), and accelerated electrons (red) at different times: side view (a) and front view (b). Magnets are outlined in red, MCP in green, and steel plates in yellow

Table 1 shows the data obtained during the simulation related to the specified offset of the trajectory of the electron beam with $E_k = (33.9 \pm 0.3)$ keV from the center of the magnets along the Y-axis and the presence of suppressive steel plates (see Figs. 5, 6). Also the values of the maximum scatter distance S between electrons at a distance of 190 mm (see Fig. 6) after the magnets are presented. In addition, the values of the divergence angle α between the maximally accelerated and decelerated electrons after bending the trajectory of their motion by 90° and coming out of the magnetic field are presented.

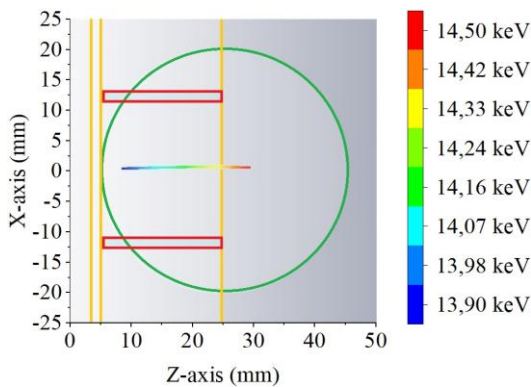


Fig. 7. Experiment simulation model (top view) showing the energy distribution of deflected electrons with $E_k = (14.2 \pm 0.3)$ keV on the MCP surface

As you can see from Table 1, electrons with different energies have a larger divergence angle when moving along the periphery of the magnetic field, where it is more non-uniform than in the center. Steel plates suppress the magnetic field, which has the opposite direction. This feature further increases divergence of electrons at the exit from the spectrometer.

Table 1

Selection of configurations of spectrometer with the highest resolution for deflecting electrons with $E_k = (33.9 \pm 0.3)$ keV

Offset from the center of the magnets along the Y-axis, mm	Scatter distance of electrons S , mm	Divergence angle of electrons α , mrad
-2 without steel plates	2.5	13
+8 without steel plates	3.5	17
+11.4 with steel plates	4.5	22

The calculation and development of the magnetic system was carried out for three given initial energy values of electron beams that will be used in the experiment on dielectric laser acceleration. These initial energy values are associated with a fixed interval of periodic structures used to accelerate the electrons.

Table 2 shows the data obtained during the simulation related to the specified offset of the trajectory of the electron beam from the center of the magnets along the Y-axis when suppressive steel plates are present (see Figs. 5, 6). Also the values of the scatter distance S between electrons with $\Delta E_k = 600$ keV at a distance of 190 mm (see Fig. 6) after the magnets are presented. In addition, the values of the divergence angle α between the maximally accelerated and decelerated electrons after bending the trajectory of their motion by 90° and coming out of the magnetic field are presented.

Table 2

Parameters of the simulated spectrometer for deflecting electrons with different energies

Offset from the center of the magnets along the Y-axis, mm	Energy of electrons E_k , keV	Scatter distance of electrons S , mm	Divergence angle of electrons α , mrad
+11.4	33.9 ± 0.3	4.5	22
+13.9	18.2 ± 0.3	14.3	71
+14.6	14.2 ± 0.3	19.4	96

As you can see in Table 2, for all electron energies sufficient divergence is achieved and electrons do not go beyond the MCP boundaries without changing the spectrometer configuration.

CONCLUSIONS

The proposed scheme, in which the electron beam passes along the periphery of the magnetic field between a pair of permanent magnets, rather than through the center of the magnetic electron spectrometer as in [7, 8], provides an opportunity to significant increase the divergence angle between electrons with different energies without increasing the dimensions of the deflection system. This is attributed to three reasons. Firstly, path length of all electrons within the magnetic field is increased. Secondly, electrons with lower energy enter the region with higher magnetic induction faster compared to electrons with higher energy, further increasing the difference in Larmor radii (2) as electrons with different energies move along the periphery of the magnetic field (see Fig. 3,b,c). Thirdly, steel plates sup-

press the magnetic field with an opposite direction along the path of the electrons (see Fig. 3,c). Using such a scheme in real experiments, under otherwise equal conditions, will enhance the precision of the energy measuring without the need for additional registration devices or reducing the transverse width of the electron beam.

Simulation results also indicated that the precision of magnet positioning should be no less than 0.1 mm for the selected magnets and energies of electrons.

ACKNOWLEDGEMENTS

The study is supported by the National Research Foundation of Ukraine under the program “Leading and Young Scientists Research Support” (project № 2020.02/0299).

REFERENCES

1. M. Galimberti, A. Giuliotti, D. Giuliotti, L.A. Gizzi. SHEEBA: A spatial high energy electron beam analyzer // *Review of scientific instruments*. 2005, v. 76, p. 053303. <https://doi.org/10.1063/1.1899309>.
2. N.I. Tarantin. *Magnetic static analyzers of charged particles*. M.: “Energoatompubl”, 1986, p. 10.
3. C.M.S. Sears, S.B. Cuevas, U. Schramm, K. Schmid, A. Buck, D. Habs, F. Krausz, L. Veisz. A high resolution, broad energy acceptance spectrometer for laser wakefield acceleration experiments // *Review of scientific instruments*. 2010, v. 81, p. 073304. <http://doi.org/10.1063/1.3458013>.
4. R.J. England, U. Niedermayer, L. Schachter, T. Hughes, P. Musumeci, R.K. Li, W.D. Kimura. Considerations for a TeV collider based on dielectric laser accelerators // *JINST*. 2022, v. 17, p. 05012. <http://doi.org/10.1088/1748-0221/17/05/P05012>.
5. K.P. Wootton, J. McNeur, K.J. Leedle. Dielectric Laser Accelerators: Designs, Experiments, and Applications // *Reviews of Accelerator Science and Technology*. 2016, v. 9, p. 105-126. <https://doi.org/10.1142/S179362681630005X>.
6. J. Breuer. *Dielectric laser acceleration of non-relativistic electrons at a photonic structure*: Diss. Ludwig-Maximilians University, 2013.
7. K. Soong. *Particle accelerator on a wafer: demonstration of electron acceleration and diagnostics with microstructures*: Diss. Stanford University, 2014p. 37-38.
8. P. Yousefi. *Novel Silicon Nano-Structures for Dielectric Laser Accelerators*: Diss. Friedrich-Alexander University, 2019, p. 56-58.
9. V. Vasylyev, O. Bolshov, K. Galaydych, A. Povrozin, G.V. Sotnikov. Influence of the profile of the dielectric structure on the electric fields excited by a laser in dielectric accelerators based on chip // *Proc. 12th Int. Particle Acc. Conf. IPAC*. 2021, p. 2026-2029. <http://doi.org/10.18429/JACoW-IPAC2021-TUPAB247>.
10. F. Chen Francis. *Introduction to Plasma Physics and Controlled Fusion*. Los Angeles: “Springer International Publishing”, 2015, p. 20.
11. R.C. Fernow. *Principles of Magnetostatics*. Cambridge: “Cambridge University Press”, 2022, p. 211-228.
12. How do you calculate the magnetic flux density? // <https://www.supermagnete.de/eng/faq/How-do-you-calculate-the-magnetic-flux-density>.
13. A.V. Vasylyev, A.O. Bolshov, K.V. Galaydych, A.I. Povrozin, G.V. Sotnikov. Acceleration of electron bunches using periodic dielectric structures with and without coating // *Problems of Atomic Science and Technology*. 2021, № 4, p. 60-64. <http://doi.org/10.46813/2021-134-060>.

Article received 17.10.2023

МОДЕЛЮВАННЯ ВІДХИЛЯЮЧОЇ СИСТЕМИ НА ОСНОВІ ПОСТІЙНИХ МАГНІТІВ З НЕОДНОРІДНИМ МАГНІТНИМ ПОЛЕМ ДЛЯ РЕЄСТРАЦІЇ ПРИСКОРЕНИХ ТА СПОВІЛЬНЕНИХ ЕЛЕКТРОНІВ, ГЕНЕРОВАНИХ У ДІЕЛЕКТРИЧНОМУ ЛАЗЕРНОМУ ПРИСКОРЮВАЧІ

I.V. Безносенко, A.V. Васильєв, Г.В. Сотніков

Для просторового розділення пучка електронів з різною енергією в діапазоні кількох десятків кілоелектронвольт була розроблена та розрахована система відхилення. Для експериментів з використанням діелектричних лазерних прискорювачів були досліджені три конкретні випадки з енергіями електронів: $(33,9 \pm 0,3)$, $(18,2 \pm 0,3)$ і $(14,2 \pm 0,3)$ кеВ. Наведено результати розрахунків просторового розподілу магнітного поля, індукованого парєю постійних магнітів, і його впливу на електрони, що рухаються у цьому полі. Такі магнітні спектрометри відрізняються від своїх аналогів тим, що частинки рухаються не по центру між магнітами в однорідному магнітному полі, а по їх периферії, де поле неоднорідне, що забезпечує більш високу роздільну здатність. Представлений спектрометр забезпечує енергетичну роздільну здатність електронів менше 10 еВ. Дослідження таких систем має важливе значення для подальшого розвитку методів аналізу електронів із змінюваною енергією в сучасних прискорювачах і спектрометрах.